

Hydrothermal syntheses, structures and luminescent properties of Zn(II)
coordination polymers assembled with benzene-1,2,3-tricarboxylic acid
involving in situ ligand reactions

Wenlong Liu,^{*a,b} Jianghua Yu,^a Jiaxun Jiang,^a Limin Yuan,^a Bin Xu,^a Qiang Liu,^a Botao Qu,^a
Guoqing Zhang^a and Chaoguo Yan^{*a}

^a College of Chemistry and Chemical Engineering, Yangzhou University, Yangzhou, 225002, China. Fax: 86 514 87975244; Tel: 86 514 87975290; E-mail: liuwl@yzu.edu.cn.

^b State Key Laboratory of Coordination Chemistry, Nanjing University, China.

Electronic Supporting Information

Page S2: Table S1 Selected bond lengths (Å) and angles (°) for complexes **1-5**

Page S3: Table S2 Hydrogen Bonds (Å, °) for **1**.

Table S3 The dihedral angles of different coordination conformations in compounds **1-5** and **R1**

Table S4 The statistics of the powder XRD preferred orientation for compounds **1-5**

Page S4: Fig. S1 (a) An illustration of the bimetallic 26-member ring in **1**. (b) Packing diagram of the 3D network of **1** viewed down the crystallographic *a*-axis.

Fig. S2 (a) The interactions between C6 and the imidazole rings of bix ligands in **2**. (b) View of the 3D supramolecular framework through C-π between 2D layers of **2**.

Page S5: Fig. S3 (a) A 1D double chain composed of Zn1 and 1,2,3-btc³⁻. (b) 3D network pillared by 4,4'-bpy ligands in **3**.

Fig. S4 The coordination conformations of bbi in **4**.

Page S6: Fig.S5 (a) Two helical array (*RL*) and (*LR*) go to two different directions. (b) View of the 3D network constructed from [Zn₃(1,2,3-btc)₂] layers (red ones) and bbi helical chains. (c) 3D porous framework of **4**.

Fig. S6 (a) View of the 1D double *meso*-helical chain. (b) View of the 3D supramolecular framework through C-H...π interactions. (C) and (d) The C-H...π interactions between 1D chains in **5**.

Page S7: Fig. S7 Simulated and experimental XRPD patterns of **1-5**.

Page S8-S9: Fig. S8 The final Rietveld refinement plots of **1** (a), **2** (b), **3** (c), **4** (d) and **5** (e)

Page S10: Fig.S9 TG curves of complexes **1-5**.

Page S11: Fig. S10 TGA curve for **2** from RT to 1200°C in nitrogen environment

Page S11: Fig. S11 TGA curve for **5** from RT to 1375°C in nitrogen environment

Page S11-S12: The high temperature TGA and ZnO ex-situ analysis

Table S1 Selected bond lengths (Å) and angles (°) for complexes **1–5^a**

1					
Zn1-O1	1.943(2)	Zn1-O4#1	1.966(2)	Zn1-N1	1.988(2)
Zn1-N4 #2	1.997(2)	O1-Zn1-O4#1	115.86(8)	O1-Zn1-N1	114.68(8)
O4#1-Zn1-N1	99.33(7)	O1-Zn1-N4#2	110.52(9)	O4#1-Zn1- N4#2	100.92(8)
N1-Zn1-N4#2	114.42(8)				
2					
Zn1-O5#1	1.947(2)	Zn1-O1	1.957(2)	Zn1-N3	2.024(3)
Zn1-N1	2.039(3)	O1-Zn1-O5#1	130.13(10)	O5#1-Zn2-N3	106.94(10)
O1-Zn1-N3	103.59(10)	O5#1-Zn1-N1	96.32(10)	O1-Zn1-N1	110.91(10)
N3-Zn1-N1	107.544(11)				
3					
Zn1-O3	1.981(5)	Zn1-O5#2	1.957(6)	Zn1-O2#1	1.942(5)
Zn1-N1	2.005(6)	Zn2-O7	2.066(9)	Zn2-O8	2.123(11)
Zn2-N2#3	2.138(7)	Zn2-O1	2.161(5)	O2#1-Zn1-O5#2	129.3(3)
O2#1-Zn1-O3	95.2(2)	O5#2-Zn1-O3	98.7(2)	O2#1-Zn1-N1	113.5(2)
O5#2-Zn1-N1	104.3(3)	O3-Zn1-N1	114.5(2)	O7-Zn2-O8	180.00(1)
O7-Zn2-N2#3	92.3(2)	O8-Zn2-N2#3	87.7(2)	O7-Zn2-O1	90.18(15)
O8-Zn2-O1	89.82(15)	N2#3-Zn2-O1	92.1(2)	N2#4-Zn2-O1	87.9(2)
O1#5-Zn2-O1	179.6(3)	N2#3-Zn2-N2#4	175.4(4)		
4					
Zn1-O1	1.985(3)	Zn1-O11#1	1.986(3)	Zn1-N1	2.001(4)
Zn1-N5	2.023(4)	Zn2-O6	1.968(3)	Zn2-N9	1.991(4)
Zn1-O1	1.950(3)	Zn2-O5#2	1.936(3)	Zn2-O9	2.019(3)
Zn2-N7#2	2.051(4)	Zn3-O7	1.980(3)	Zn3-N3#3	2.011(4)
Zn3-N11#1	2.041(4)	Zn3-O4#4	2.233(4)	Zn3-O3#4	2.233(4)
O1-Zn1-O11#1	124.98(13)	O1-Zn1-N1	107.06(14)	O11#1-Zn1-N1	105.16(13)
O1-Zn1-N5	96.48(13)	O11#1-Zn1-N5	11.42(14)	N1-Zn1-N5	111.48(15)
O6-Zn2-N9	123.71(14)	O6-Zn2-O9	110.17(12)	N9-Zn2-O9	113.38(14)
O6-Zn2-N7#2	101.58(14)	N9-Zn2-N7#2	104.77(15)	O9-Zn2-N7#2	99.21(13)
O7-Zn3-N3#3	105.20(14)	O7-Zn3-N11#1	94.35(14)	N3#3-Zn3-N11#1	103.17(16)
O7-Zn3-O4#4	101.60(12)	N3#3-Zn3-O4#4	146.81(15)	N11#1-Zn3-O4#4	93.88(14)
O7-Zn3-O3#4	134.33(13)	N3#3-Zn3-O3#4	88.22(14)	N11#1-Zn3-O3#4	125.37(14)
O4#4-Zn3-O3#4	58.86(13)				
5					
Zn1-O1	1.946(2)	Zn1-O4#1	1.963(2)	Zn1-N3#2	1.999(2)
Zn1-N1	2.018(2)	O1-Zn1-O4#1	117.37(8)	O1-Zn1-N3#2	110.71(8)
O4#1-Zn1-N3#2	106.53(9)	O1-Zn1-N1	114.51(8)	O4#1-Zn1-N1	92.83(8)
N3#2-Zn1-N1	113.71(9)				

^aSymmetry codes, For **1**: #1 x-1,y,z; #2 -x,-y,-z. For **3**: #1 x,y-1,z. For **4**: #1 -x+1/2,y+1/2,-z+1/2; #2 -x+1/2,y-1/2,-z+1/2; #3 -x+1/2,-y+3/2,-z; #4 x+1/2,-y+3/2,z+1/2; #5 -x+1,y,-z+1/2. For **5**: #1 -x+1,y+1/2,-z+3/2; #2 x,-y+1/2,z-1/2; #3 -x+2,-y,-z+2; #4 x-1,y,z. For **6**: #1 x+1,-y-1/2,z+1/2; #2 x-1,-y-1/2,z-1/2.

Table S2 Hydrogen Bonds (Å, °) for **1**

D–H...A	r (D–H)	r(H...A)	r(D...A)	α(D–H...A)	Symmetry operation
O5–H5...N6	0.8200	1.8000	2.604(4)	167.00	1-x,1-y,1-z
C4–H4...O3	0.9300	2.4400	2.752(4)	100.00	
C6–H6...O1	0.9300	2.3900	2.719(3)	100.00	
C10–H10...O2	0.9300	2.4100	3.091(4)	130.00	
C11–H11...O5	0.9300	2.5900	3.512(4)	173.00	-1+x, y, z
C13–H13B...O4	0.9700	2.5200	3.419(5)	153.00	1-x,1-y,-z
C15–H15...O1	0.9300	2.5800	3.472(4)	160.00	-x,1-y,-z
C16–H16...O3	0.9300	2.5600	3.378(4)	147.00	-1+x,y,-1+z
C20–H20A...O3	0.9700	2.4300	3.260(4)	143.00	-1+x,y,-1+z
C20–H20B...O1W	0.9700	2.5700	3.453(9)	151.00	1-x,1-y,-z
C21–H21...O6	0.9300	2.4200	3.279(4)	154.00	1-x,-y,-z
C23–H23...O3	0.9300	2.6000	3.294(4)	132.00	-1+x,y,-1+z
C24–H24...O5	0.9300	2.4100	3.255(4)	151.00	x,y,1+z

Table S3 The dihedral angles of different coordination conformations in compounds **1–5** and **R1**

Plane1	Plane2	a	b	c	e	d
phenyl ring	CG1	19.673(13)	30.790(5)	60.517(8)	55.500(6)	6.163(2)
phenyl ring	CG2	82.736(26)	69.515(8)	64.240(8)	50.076(5)	80.295(8)
phenyl ring	CG3	11.794(2)	33.630(5)	47.742(5)	50.519(6)	25.266(5)
CG1 ^a	CG3	29.908(3)	59.052(5)	87.465(12)	83.955(12)	30.198(5)
CG1	CG2	77.439(22)	59.573(8)	54.424(8)	54.615(8)	86.165(8)
CG2	CG3	77.885(27)	62.358(10)	53.941(8)	50.239(8)	67.852(6)

^aCG represent carboxylate group.

Table S4 The statistics of the powder XRD preferred orientation for compounds **1–5**

Sample	Dir 1			Dir 2		Fraction of Dir 1		
	H	K	L	H	K			
1	0	0	1	0.8509154	0	3	0	0.3385876
2	1	1	0	0.8178393	0	0	2	0.8006425
3	0	0	2	0.6329221	1	-1	-1	0.8582032
4	0	1	1	0.1159393	1	0	1	0.02893791
5	0	2	0	0.1366501	1	1	0	0.1099115

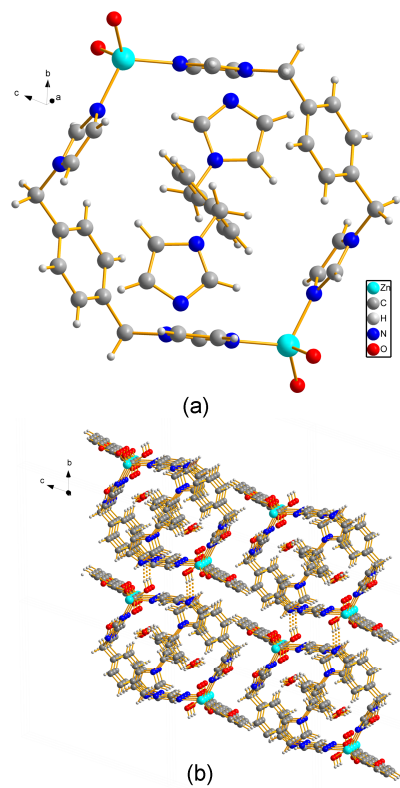


Fig. S1 (a) An illustration of the bimetallic 26-member ring in **1**. (b)Packing diagram of the 3D network of **1** viewed down the crystallographic *a*-axis.

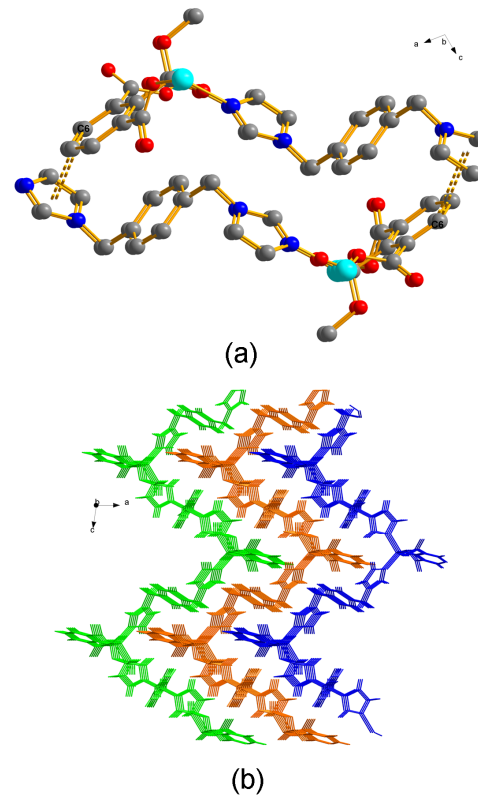
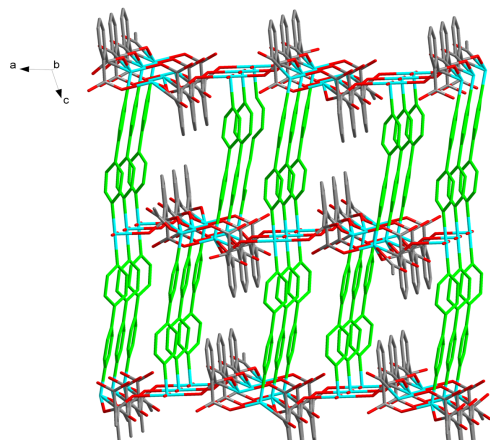


Fig. S2 (a) The interactions between C6 and the imidazole rings of bix ligands in **2**. (b) View of the 3D supramolecular framework through C- π between 2D layers of **2**.



(a)



(b)

Fig. S3 (a) A 1D double chain composed of Zn1 and 1,2,3-btc³⁻. (b) 3D network pillared by 4,4'-bpy ligands in **3**.

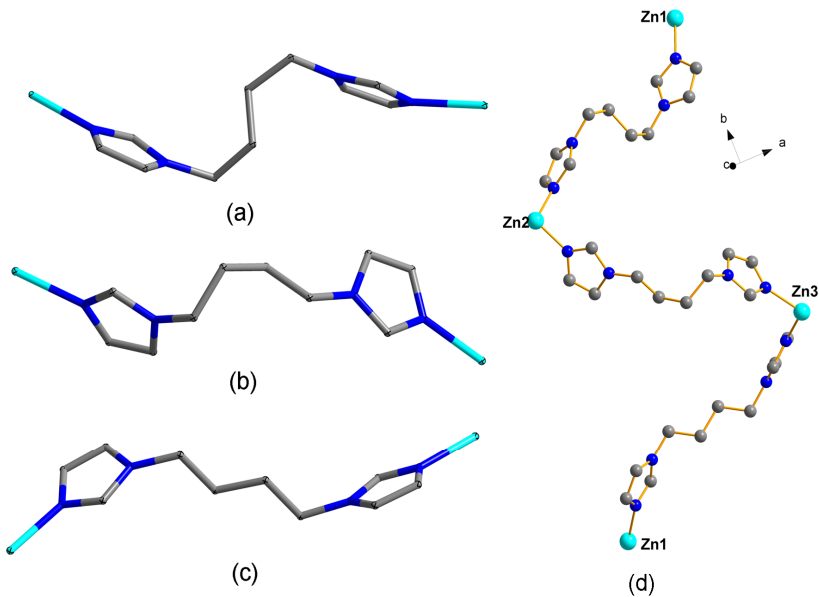


Fig. S4 The coordination conformations of bbi in **4**.

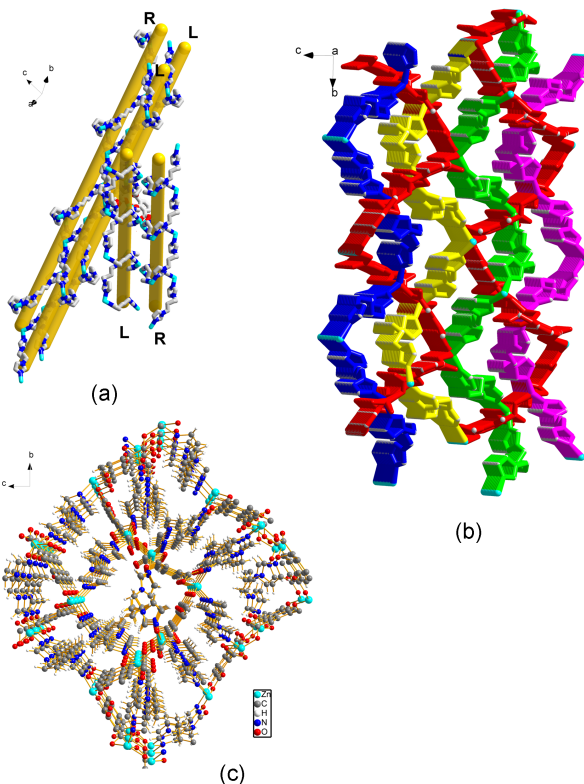


Fig.S5 (a) Two helical array (*RL*) and (*LR*) go to two different directions. (b) View of the 3D network constructed from $[Zn_3(1,2,3\text{-btc})_2]$ layers (red ones) and bbi helical chains. (c) 3D porous framework of **4**.

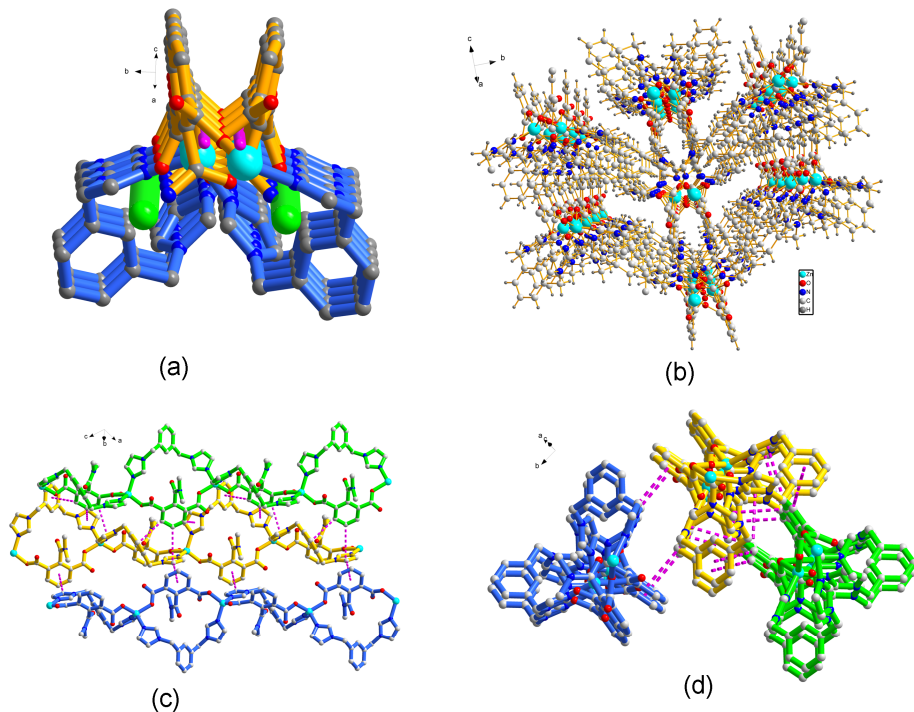


Fig. S6 (a)View of the 1D double *meso*-helical chain. (b) View of the 3D supramolecular framework through C–H... π interactions. (C) and (d) The C–H... π interactions between 1D chains in **5**.

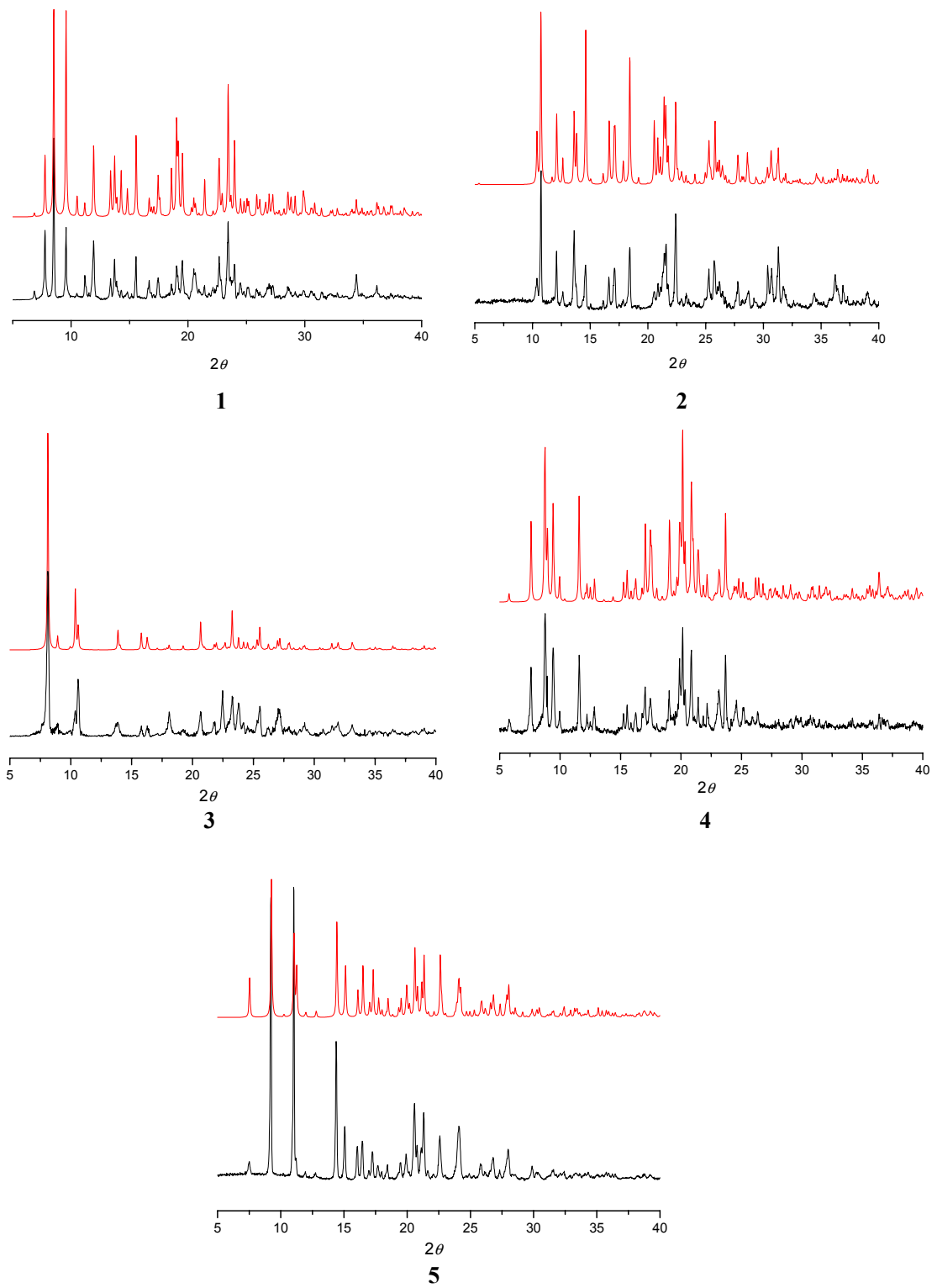
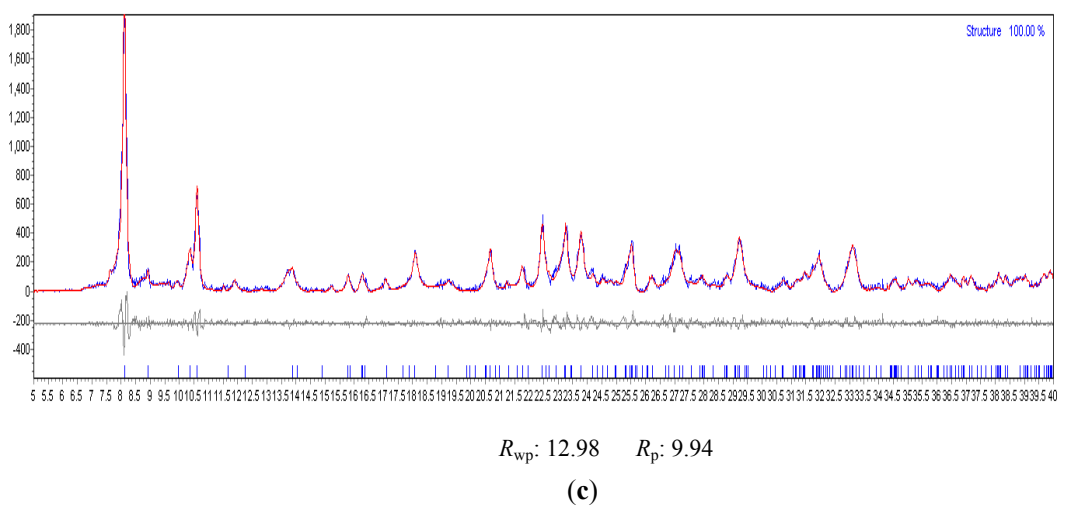
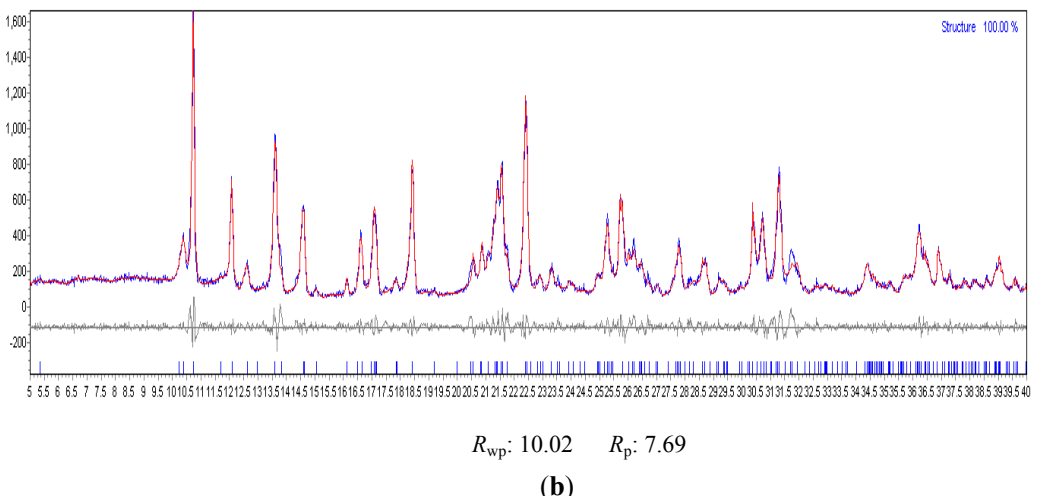
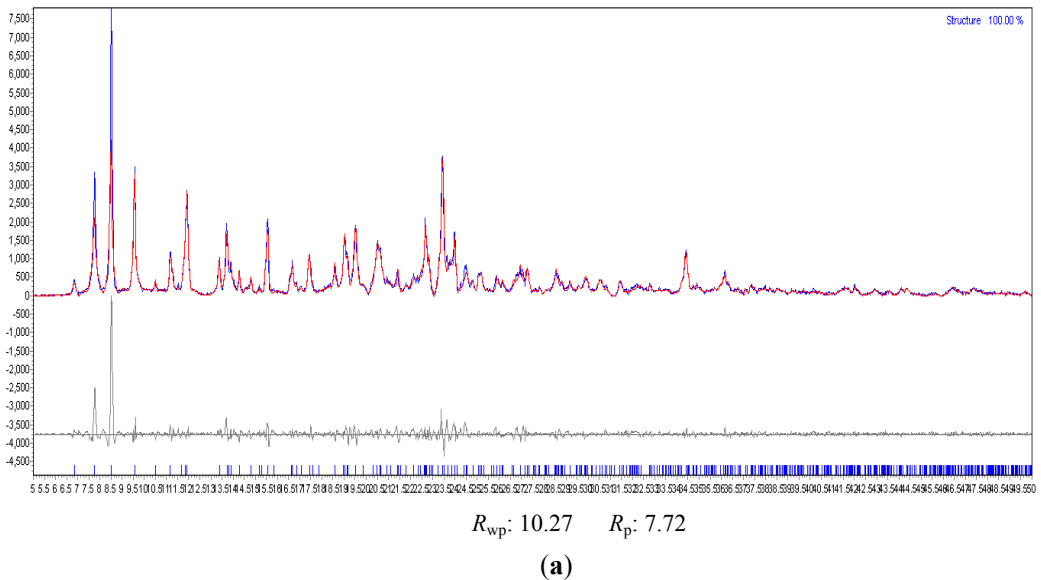
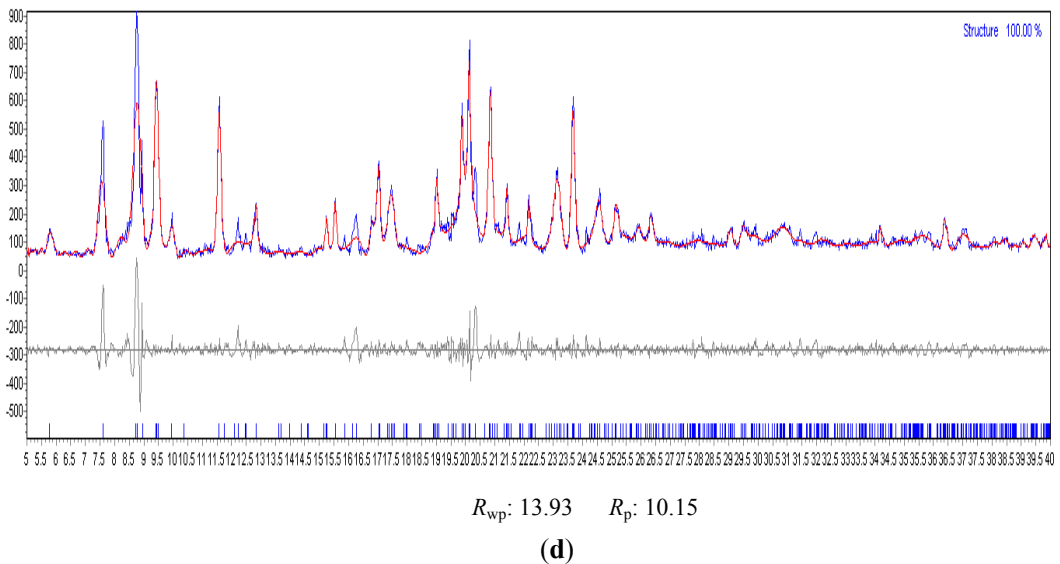
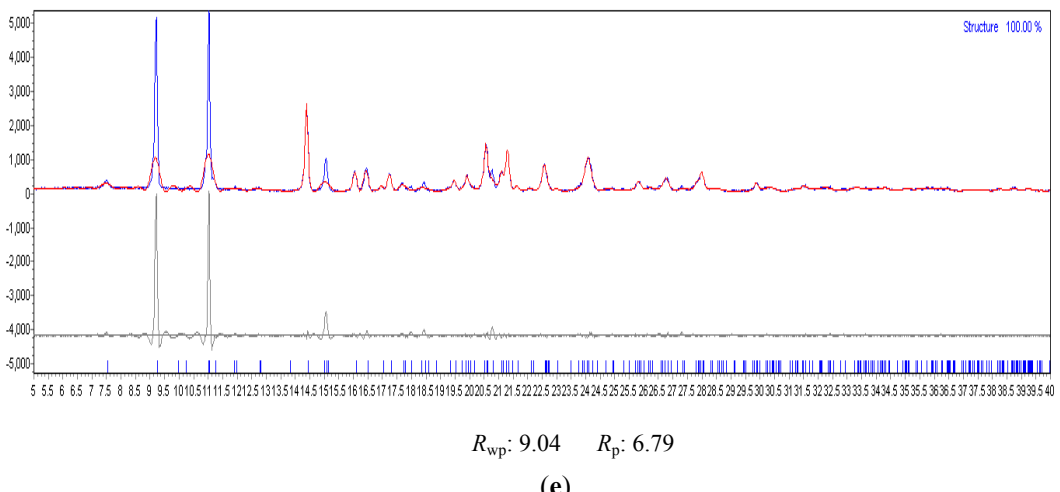


Fig. S7 Simulated(red) and experimental XRPD patterns of 1-5.





(d)



(e)

Fig. S8 The final Rietveld refinement plots of **1** (a), **2** (b), **3** (c), **4** (d) and **5** (e): experimental pattern (blue), calculated pattern (red), and difference profile (bottom gray line). Stick marks (|) at the bottom of the pattern indicate peak positions allowed by the unitcell parameters and space group.

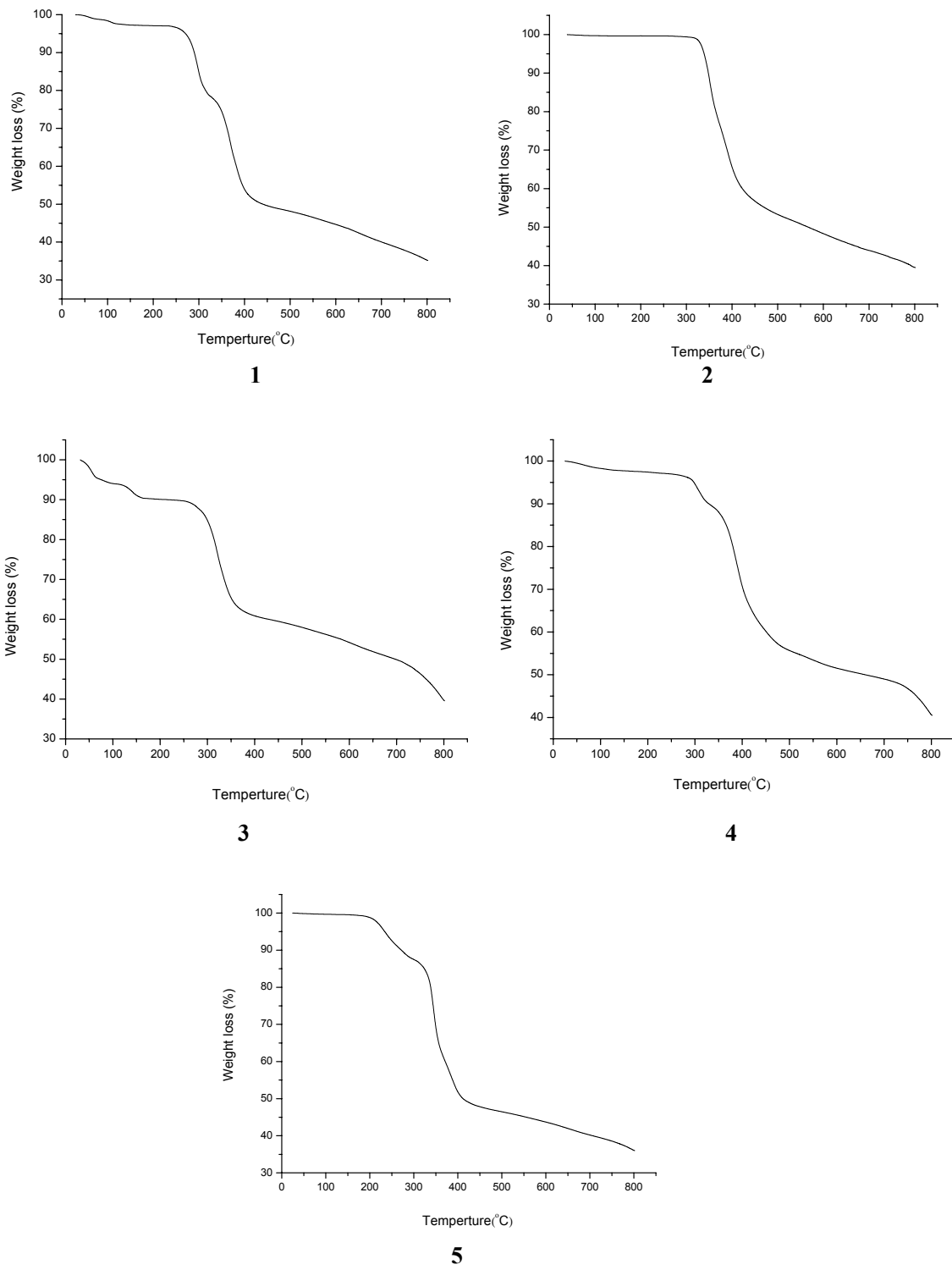


Fig. S9 TG curves of complexes **1-5**.

The high temperature TGA and ZnO ex-situ analysis

The high temperature TGA experiments in nitrogen environment were carried out for compound **2** and **5** (see following Fig. S10 and Fig. S11). As shown in following Figures, the curves are same as the results of prior experiments before 800°C, but a continuous weight loss occurred from 800 to 1200°C for **2**, without a definite endpoint in the experiments, even if the temperature to 1400°C for **5**. The decomposition mechanisms might be the carboreduction in nitrogen environment. The organic ligands were decomposed to CO or C in nitrogen environment, then CO or C reduced the ZnO to Zn at higher temperture. The boiling point of metallic Zn is 907°C.



Similar researches have been reported.¹⁻³

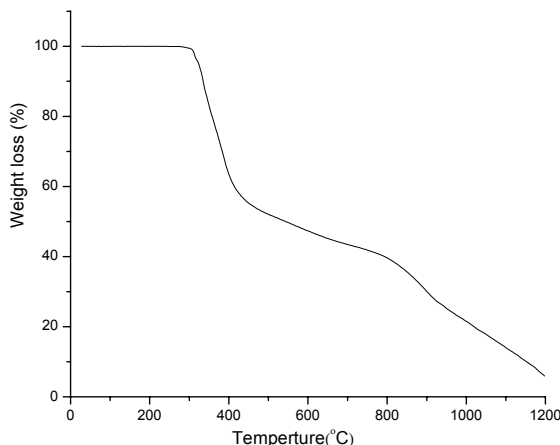


Fig. S10 TGA curve for **2** from RT to 1200°C in nitrogen environment

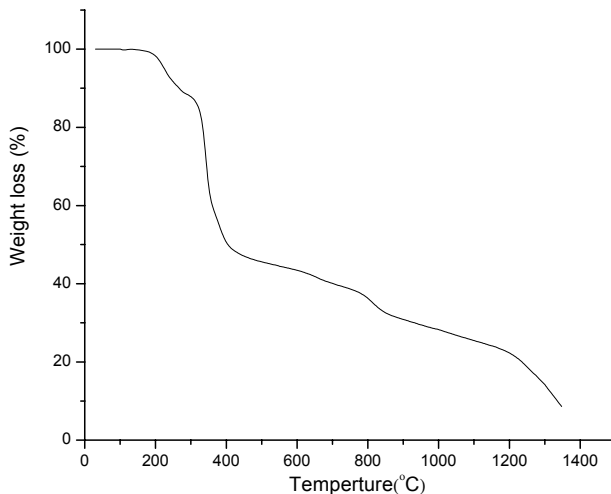


Fig. S11 TGA curve for **5** from RT to 1375°C in nitrogen environment

Because the amount of remaining residue after TGA is small (about 2 mg), we can not to characterize them by powder XRD. In order to decompose samples to ZnO and confirm the sample purity, about 200 mg samples were placed in a Muffle Furnace, which were heated at 800°C for 2 hr in air. Gravimetric analysis was used to analyze the ZnO contents. The results are listed in following Table S5. The purity of remaining residue was confirmed by x-ray diffraction (Fig. S12).

Table S5 The results of ZnO contents by Gravimetric analysis

Sample	Weight (mg)		ZnO(%)	
	Start	After heated	Observed	Calculated
1	203.8	25.7	12.61	12.54
2	211.5	32.9	15.56	15.48
3	201.3	48.3	23.99	23.89
4	208.8	42.4	20.31	20.21
5	213.2	28.4	13.32	13.29

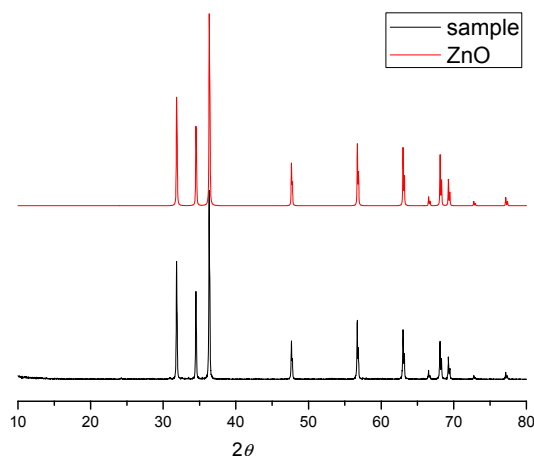


Fig. S12 The powder XRD pattern of the remaining residue after heated at 800°C for 2 hr in air.

References

1. J. V.D.S. Araújo, R.V. Ferreira, M. I. Yoshida and V. M. D. Pasa, *Solid State Sci.*, 2009, **11**, 1673.
2. M. H. Huang, S. Mao, H. Feick, H. Yan, Y. Wu, H. Kind, E. Weber, R. Russo, and P. Yang, *Science*, 2001, **292**, 1897.
3. K. Subannajui, N. Ramgir, R. Grimm, R. Michiels, Y. Yang, S. Müller and M. Zacharias *Cryst. Growth Des.*, 2010, **10**, 1585.